

Effects of Spin Fluctuations in Quasi-One-Dimensional Organic Superconductors

Hiori KINO and Hiroshi KONTANI¹

Joint Research Center for Atom Technology, Tsukuba, Ibaraki, 305-0046,

¹*Institute for Solid State Physics, University of Tokyo, 7-22-1 Roppongi, Minato-ku, Tokyo 106-8666.*

(Received February 23, 1999)

We study the electronic states of quasi-one-dimensional organic conductors using the single band Hubbard model at half-filling. We treat the effects of the on-site Coulomb interaction by the fluctuation-exchange (FLEX) method, and calculate the phase diagram and physical properties. The calculated pressure dependence of the Néel temperature coincides well with the experimental one. We also show that a pseudogap is formed in the density of states near the chemical potential and that *d*-wave superconductivity appears next to the antiferromagnetic state. Moreover the NMR relaxation rate increases on cooling in the low-temperature region

KEYWORDS: quasi-one-dimensional organic conductors, Hubbard model, spin fluctuations, TMTSF, TMTTF, FLEX approximation, superconductivity, antiferromagnetism

It is known that the quasi-one-dimensional organic superconductors (TMTSF)₂X and similar compounds have very rich varieties of phases.^{1,2)} For example, (TMTTF)₂PF₆ is in the spin-Peierls phase at ambient pressure. The antiferromagnetic insulating phase is stabilized with applied pressure larger than about 10 kbar. The antiferromagnetic transition temperature, *T_N*, becomes maximum (~ 20 K) around 15 kbar. (TMTSF)₂PF₆ is in the antiferromagnetic insulating phase at ambient pressure. The antiferromagnetism disappears with increasing pressure to give rise to superconductivity. The maximum superconducting transition temperature is about 1 K. The superconducting phase is next to the antiferromagnetic one and it indicates that the spin fluctuation is closely connected with the emergence of the superconductivity. It is also very interesting that the pseudogap was observed in the density of states (DOS) near the chemical potential in XPS experiments.^{3,4)}

In the previous theoretical studies, the Hubbard model was mainly studied as the simplest model in these systems. The SDW transition temperature and phase boundary between the SDW and the superconducting phases were discussed within the mean field, or the RPA treatment.^{5,6)} Shimahara discussed the spin fluctuations as an origin of the superconductivity.⁷⁾ This work and the QMC study indicated that the superconductivity was realized and the superconducting order parameter had line-nodes on the Fermi surface.⁸⁾ Dimensional crossover was discussed based on the renormalization group theory.⁹⁾

The aim of this letter is to discuss the origin of pseudogap behavior detected in the XPS experiments, and the origin of superconductivity on the basis of the Fermi liquid theory, and to understand the phase diagrams of TMTSF and TMTTF salts. We show that these physical behaviors can be explained naturally in terms of spin-fluctuation theory. This is the first study on the

quasi-one-dimensional organic conductors where the effects of spin fluctuations are taken into account in a self-consistent way and where the antiferromagnetism and the superconductivity are treated on the same footing.

These systems have a half hole per TMTSF/TMTTF molecule in the HOMO level, and the one-dimensional chain is connected weakly.^{10,11)} The dimerization, though it is weak, exists and the antibonding band which crosses the chemical potential is half-filled.¹²⁾ Therefore we consider a single-band Hubbard model whose band dispersion is given as

$$\epsilon(k_x, k_y) = 2t_0 \cos ak_x + 2t_1 \cos bk_y + 2t_2 \cos 2bk_y, \quad (1)$$

where $|t_0| \gg |t_1| \gg |t_2|$ and *a* and *b* are the effective lattice constants. It was known that the $\cos 2bk_y$ term was necessary to appropriately reproduce the shape of the Fermi surface.⁶⁾ The physical role of this term is that it breaks the nesting condition, in other words, that it introduces frustration. It was also known that *t₂* was proportional to t_1^2/t_0 , when this term was derived from the quarter-filled Hubbard model. We study the single-band Hubbard model at half-filling and assume the screening of long range Coulomb interactions for simplicity. This is justified because the antiferromagnetic fluctuations play the essential roles.

In this study, we put $t_0 = -1$, $t_2 = 0.8t_1^2/t_0$ and the on-site Coulomb interaction $U = 3.0$, and vary $t_1 (< 0)$ as a parameter. Here $|t_2|$ is rather large compared to the model derived from the quarter-filled Hubbard model.⁶⁾ Such a choice is mainly due to the convenience of the numerical calculation because we use a finite **k**-mesh. We implicitly use 128×128 **k**-mesh and 256 Matsubara frequencies in this study.

To tackle the present model we employ the fluctuation exchange (FLEX) method, which is a kind of self-consistent perturbation theory with respect to *U*. The FLEX method has been considered to be advantageous

for systems with large spin fluctuations. It was known that this method gave the Green function which agreed with the QMC one for the square-lattice Hubbard model with moderate U .¹³⁾ This method was applied to the study of high- T_c cuprates, superconducting ladder compounds and κ -(BEDT-TTF) salts and so on,^{14,15,16)} and predicted the possible d -wave superconductivity. The QMC study also supported this result.^{8,17)}

Here, we explain the FLEX method. The Dyson equation is written as

$$\{G(\mathbf{k}, \epsilon_n)\}^{-1} = \{G^0(\mathbf{k}, \epsilon_n)\}^{-1} - \Sigma(\mathbf{k}, \epsilon_n), \quad (2)$$

where $G^0(\mathbf{k}, \epsilon)$ is the unperturbed Green function. The self-energy at temperature T is given by

$$\Sigma(\mathbf{k}, \epsilon_n) = T \sum_{\mathbf{q}, l} G(\mathbf{k} - \mathbf{q}, \epsilon_n - \omega_l) \cdot U^2 \times \left(\frac{3}{2} \chi^{(-)}(\mathbf{q}, \omega_l) + \frac{1}{2} \chi^{(+)}(\mathbf{q}, \omega_l) - \chi^0(\mathbf{q}, \omega_l) \right), \quad (3)$$

$$\chi^{(\pm)}(\mathbf{q}, \omega_l) = \chi^0(\mathbf{q}, \omega_l) \cdot \{1 \pm U \chi^0(\mathbf{q}, \omega_l)\}^{-1}, \quad (4)$$

$$\chi^0(\mathbf{q}, \omega_l) = -T \sum_{\mathbf{k}, n} G(\mathbf{q} + \mathbf{k}, \omega_l + \epsilon_n) G(\mathbf{k}, \epsilon_n), \quad (5)$$

where $\epsilon_n = (2n+1)\pi T$ and $\omega_l = 2l\pi T$. Equations (2)-(5) are calculated together with the equation for the chemical potential μ given by $N = 2T \sum_{\mathbf{p}, n} G(\mathbf{p}, \epsilon_n) e^{i\epsilon_n 0^+}$, where $N = 1$ in this system.

To determine the magnetic transition temperature T_N , we calculate the Stoner factor without vertex corrections, $\alpha_S = \max_{\mathbf{k}} \{ U \cdot \chi^0(\mathbf{k}, \omega=0) \}$. The antiferromagnetic critical points are determined by the Stoner criterion, $\alpha_S = 1$.

We also determine the superconducting transition temperature T_c by solving the linearized Eliashberg equation with respect to the singlet-pairing order parameter, $\phi(-\mathbf{k}, \epsilon_n) = +\phi(\mathbf{k}, \epsilon_n)$,

$$\lambda \cdot \phi(\mathbf{k}, \epsilon_n) = -T \sum_{\mathbf{q}, m} V(\mathbf{k} - \mathbf{q}, \epsilon_n - \epsilon_m) \times G(\mathbf{q}, \epsilon_m) G(-\mathbf{q}, -\epsilon_m) \cdot \phi(\mathbf{q}, \epsilon_m), \quad (6)$$

$$V(\mathbf{k}, \omega_l) = \frac{3}{2} U^2 \chi^{(-)}(\mathbf{k}, \omega_l) - \frac{1}{2} U^2 \chi^{(+)}(\mathbf{k}, \omega_l) + U, \quad (7)$$

where T_c is given by the condition $\lambda = 1$.

The theories by Mermin and Wagner, and Hohenberg prohibit finite T_N and T_c in two dimensions. It was well known that α_S satisfies this condition, because FLEX treats the spin fluctuations self-consistently.¹⁸⁾ We estimate T_N by the condition $\alpha_S = \alpha_N$, where $(1 - \alpha_N)^{-1} \sim O(100)$. This implies that the weak magnetic coupling between layers J_\perp makes the system ordered three-dimensionally. On the other hand, $\lambda = 1$ is fulfilled at finite T_c using eq. (6). However the T_c given by the Eliashberg equation is reliable in many cases.

First, let us examine the phase diagram on the plane of $|t_1|$ and T . Each line corresponds to T_N for different α_N . With increasing $|t_1|$ ($\lesssim 0.3$) T_N increases gradually and has a broad peak ($T_N \sim 0.4$) around $|t_1| = 0.3$. On the other hand, T_N decreases rather rapidly with increasing $|t_1|$ ($\gtrsim 0.4$). This behavior is consistent with experi-

ments if one regards $|t_1|$ as applied pressure. We do not have a plot for $|t_1| < 0.1$, where \mathbf{k} -mesh and Matsubara frequencies are insufficient to determine T_N numerically.

An inset of Fig. 1 shows the phase diagram at $U = 1.8$ where $\chi(\mathbf{q}, \omega)$ is calculated using $G^0(\mathbf{k}, \omega)$ and the Néel temperature is estimated by the Stoner criterion, $\alpha_N = 1$. The value of U is chosen in order to make T_N drop at $|t_1| \sim 0.4$. In this case T_N does not descend with decreasing $|t_1|$. Therefore the decrease of T_N for small $|t_1|$ in Fig. 1 is due to the self-consistency. We note that the estimated T_N using $G^0(\mathbf{k}, \omega)$ is about 10 times larger than that using self-consistent $G(\mathbf{k}, \omega)$, at $t_1 = -0.3$ and $U = 3.0$.

Fig. 1. The Néel temperature, T_N , determined self-consistently as a function of $|t_1|$ at $U = 3.0$, and $\alpha_N = 0.992$ (square) and $\alpha_N = 0.994$ (circle). An inset shows the T_N using G^0 in χ at $U = 1.8$. The incommensurate region corresponds to the closed symbols.

In this model, the nesting vector \mathbf{Q} is commensurate, or (π, π) , except in the large $|t_1|$ and small T region. In Fig. 1 the incommensurate region corresponds to the closed circles and squares for $T \lesssim 0.02$. The nesting vector is incommensurate in the k_y direction, but on the other hand it is always commensurate in the k_x direction whereas the RPA result is not.^{6,19)} In other words, the SDW phase is locked to π in the k_x direction. This result is consistent with the experimental nesting vector^{20,21)} and is first realized in the self-consistent calculation. We note that the nesting vector depends on the details of the Fermi surface. Therefore it is necessary to use a realistic Fermi surface in order to compare the calculated nesting vector with the experimental one for all regions of the phase diagram.

Next let us see the Fermi surface. The Fermi surface in the present model is flatter near $k_x \sim \pm\pi$ and pointed near $k_x \sim 0$ due to the $\cos(2bk_y)$ term. In Fig. 2, the Fermi surface is shown at $t_1 = -0.4$, and $T = 0.05$ and $U = 3.0$. The Fermi surface with interaction has a smaller band dispersion in the k_y direction, at the same time, the nesting condition is better than the one without interaction.

Fig. 2. Fermi surfaces at $U = 3.0$ (a solid line) and $U = 0$ (a broken line) at $t_1 = -0.4$ and $T = 0.05$.

We plot the DOS in Fig. 3. The pseudogap emerges near the chemical potential due to the spin fluctuations and it evolves with decreasing $|t_1|$ and T . This result has close connection with the pseudogap near the chemical potential found in the XPS and ARPES experiments.^{3,4)} We note that this model is effective near the chemical potential.

We also show the uniform spin susceptibility ($\chi^-(0, \omega=0)$) and the NMR relaxation rate $((T_1 T)^{-1} = \sum_k \lim_{\omega \rightarrow 0} \text{Im } \chi^-(k, \omega)/\omega)$ in Fig. 4. With decreasing temperature, the uniform spin susceptibility decreases gradually and this behavior reflects the evolution of the pseudogap in the DOS near the chemical poten-

Fig. 3. (a) The density of states at $t_1 = -0.4$ and $U = 3.0$, and $T = 0.05$ (a solid line) and $T = 0.1$ (a broken line). and at $t_1 = -0.4$ and $U = 0$ (a dotted line). (b) The density of states at $U = 3.0$ and $T = 0.1$ and $|t_1| = 0.1, 0.2, 0.3$, and 0.4 , respectively.

tial. $(T_1 T)^{-1}$ increases with decreasing temperature in the low-temperature region. Staggered susceptibility ($\chi^-(\mathbf{Q}, \omega = 0)$) is also the case. These results seem to be consistent with experimental results.^{22, 23)}

Fig. 4. The temperature dependence of $\chi^{(-)}(0, \omega = 0)$ and $1/T_1 T$ at $t_1 = -0.4$ and $U = 3.0$.

One can calculate the Green function at lower temperature than $T \sim 0.01$, though the 256 Matsubara frequencies are not sufficient. The superconducting condition is fulfilled at $t_1 = -0.45$ and $T \lesssim 0.007$ in this model, when we use 128×128 \mathbf{k} -mesh and 512 Matsubara frequencies. We plot $\phi(k_F, 0)$ corresponding to the singlet SC order parameter in Fig. 5(a), where $T = 0.007$ and λ in eq. (6) equals 1.02. One can clearly see that nodes exist and a d -wave-like superconductivity is realized. This is consistent with the NMR experiment, which predicts the SC order parameter with line-nodes.²⁴⁾ There exists a dip at $k_y \sim 0$ and a peak at $k_y \sim \pi$. Figure 5(b) shows a contour plot of $\phi(\mathbf{k}, \omega = 0)$. At $k_y = 0$, the peak in $\phi(\mathbf{k}, \omega = 0)$ is closer to $k_x = \pi/2$ than the Fermi surface, and at $k_y = \pm\pi$ the situation is reversed. These dip and peak structures depend on the manner of warping of the Fermi surface and disappear when $|t_2|$ is small. We have checked that λ for the triplet case is about one third when the singlet SC is fulfilled. Therefore the triplet superconductivity is not realized in this model.

Fig. 5. (a) The superconducting order parameter on the Fermi surface, $\phi(k_F, \omega = 0)$, from $k_y = -\pi$ to $k_y = \pi$ and (b) the Fermi surface and the contour plot of $\phi(\mathbf{k}, \omega = 0)$, at $t_1 = -0.45$, $U = 3.0$ and $T = 0.07$.

Below we focus on the obtained phase diagram in Fig. 1. The self-consistent T_N declines with decreasing $|t_1|$, whereas the non-self-consistent T_N does not descend with decreasing $|t_1|$. At the same time, the DOS at the chemical potential decreases with decreasing $|t_1|$ because of the strong spin fluctuations in the self-consistent calculation as shown in Fig. 3. This effect is not taken into account when one uses G^0 . These two behaviors are reasonably understood through the Kramers-Kronig relation,

$$\chi^{(-)}(\mathbf{k}, \omega = 0) = \frac{2}{\pi} \text{P} \int_0^\infty \frac{\text{Im} \chi^{(-)}(\mathbf{k}, \omega + i0)}{\omega} d\omega, \quad (8)$$

where the main contribution comes from small ω . The integrand can be written as $1/\omega \text{Im} \chi^{(-)}(\mathbf{k}, \omega) \simeq 1/\omega (\text{Im} \chi^0(\mathbf{k}, \omega)) (1 - U \chi^0(\mathbf{k}, \omega))^{-1}$ for large α_S , and

$1/\omega \text{Im} \chi^0(\mathbf{k}, +i0)$ at zero temperature is estimated as

$$\lim_{\omega \rightarrow 0} \frac{1}{\omega} \text{Im} \chi^0(\mathbf{k}, +i0) = \sum_{\mathbf{q}} \text{Im} G(\mathbf{q}, 0) \text{Im} G(\mathbf{q} + \mathbf{k}, 0). \quad (9)$$

The right-hand side of eq. (9) is roughly proportional to the square of the DOS at the Fermi level. Therefore $\chi^{(-)}(\mathbf{k}, 0)$ decreases together with the evolution of the pseudogap in the DOS near the Fermi level. This is the main reason why T_N decreases for small $|t_1|$ in Fig. 1.

One can interpret the reduction of T_N for small $|t_1|$ in Fig. 1 in connection with the $S = 1/2$ coupled chain Heisenberg model.²⁵⁾ The magnetization at $T = 0$ decreases due to the zero-point fluctuation in decreasing the interchain coupling.

On the other hand, when $|t_1|$ is large enough, then $|t_2|$ is also large, and the nesting condition itself determines T_N . Hence T_N drops rapidly as seen in the RPA and mean field calculations.

The effect of applied pressure can be considered to increase the transverse transfer integrals and the band width. But it is sufficient only to enlarge the transverse transfer integrals in order to discuss the overall phase diagram in TMTTF/TMTSF salts. Experimentally, the Néel temperature (or SDW transition temperature) increases with increasing pressure, whereas it decreases and finally drops rapidly near the phase boundary with the superconducting phase.²⁾ We have derived, for the first time, the phase diagram which coincides with the experimental one by considering the effects of the strong spin fluctuations self-consistently.

Next we compare the present results quantitatively with the experimental results. If $|t_0|$ is set to 1000 K, $T = 0.01$ correspond to 10 K. These results do not correspond well with the experimental ones because U and $|t_2|$ are rather large in the present study due to the numerical calculations. But T_N is reduced with decreasing U and with increasing $|t_2|$, and the value of t_1 at which T_N takes its maximum also behaves in a similar way. Then one can adjust U and $|t_2|$ such that T_N and t_1 are close to the experimental ones.

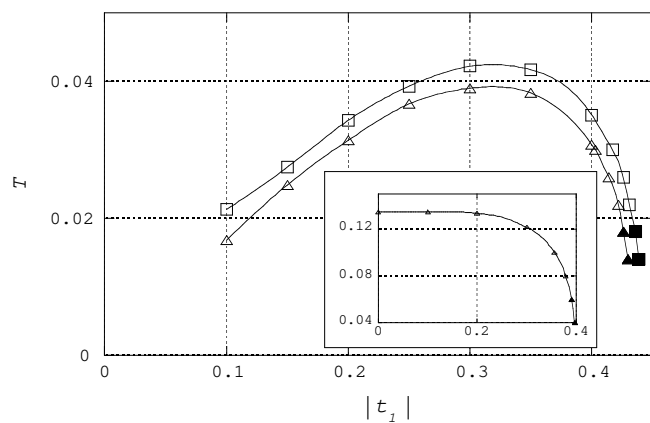
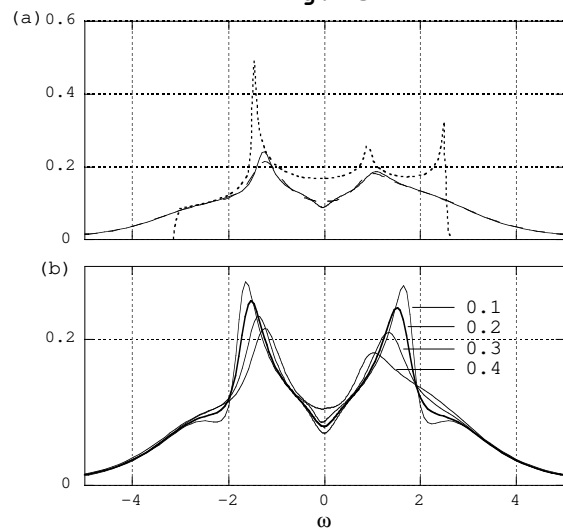
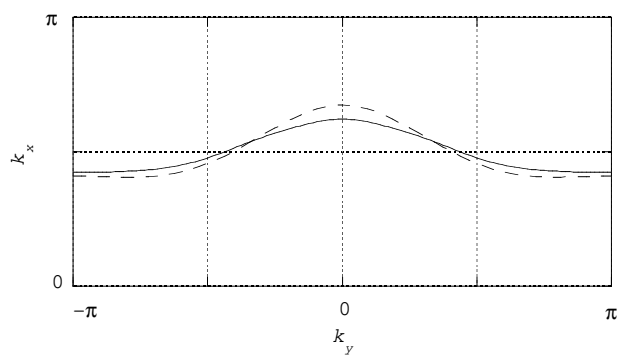
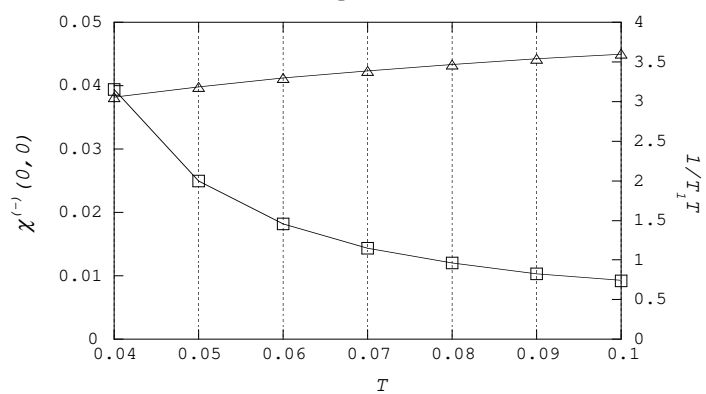
We have calculated a quasi-one-dimensional model whose lattice has zigzag hopping parameters, and have shown that the results are almost the same as that of the current model. We have also calculated the quarter-filled Hubbard model without dimerization. The temperature dependence of the Stoner factor as a function of t_1 is very similar to the case of the half-filled one in Fig. 1, i.e., T_N has a peak as a function of t_1 . But the resulting maximum T_N seems to be less than about 5×10^{-3} and the dimerization takes an important role quantitatively. These results will be published elsewhere.

The recent experiments revealed that the antiferromagnetic phases were accompanied by charge disproportionations.²⁶⁾ Naturally the importance of long-range Coulomb interactions was pointed out.^{28, 27)} The corresponding degrees of freedom, which are dropped in the current model at half-filling, will not be negligible because of the weak dimerization. Further studies including this effect are necessary in connection with the nesting vector.

In summary, we have studied the model Hamiltonian of the quasi-one-dimensional organic conductors by the FLEX method. We have successfully explained the pressure dependence of the Néel temperature as a result of the evolution of the pseudogap in the DOS near the chemical potential, and the NMR relaxation rate which increases on cooling in the low-temperature region. We have also found a d -wave-like superconductivity with line-nodes on the Fermi surface.

We are grateful to T. Takahashi, F. Aryasetiawan, N. Katoh and J. Kishine for useful discussions. We also thank Y. Kumagai for programming assistance. This work is partly supported by NEDO.

-
- [1] T. Ishiguro and K. Yamaji: *Organic Superconductors* (Springer-Verlag).
 - [2] e.g. J. Moser, *et al.*: Euro. Phys. J. B **1** 39-46 (1998).
 - [3] B. Dardel, *et al.*: Europhys. Lett. **24** 687 (1993).
 - [4] F. Zwick, *et al.*: Phys. Rev. Lett. **79** 3982 (1997).
 - [5] K. Yamaji: J. Phys. Soc. Jpn. **52** 1361 (1983).
 - [6] Y. Hasegawa and H. Fukuyama: J. Phys. Soc. Jpn. **55** 3978 (1987).
 - [7] H. Shimahara: J. Phys. Soc. Jpn. **58** 1735 (1989).
 - [8] K. Kuroki and H. Aoki: preprint (cond-mat/9812026).
 - [9] J. Kishine and K. Yonemitsu: J. Phys. Soc. Jpn. **67** 2590 (1998).
 - [10] P.M. Grant: J. Phys. Colloque (France), **44** C3-847 (1983).
 - [11] C.S. Jacobsen, D.B. Tanner, and K. Bechgaard: Phys. Rev. B **28** 7019 (1983).
 - [12] K. Penc and F. Mila: Phys. Rev. B **50** 11429 (1994).
 - [13] N.E. Bickers and S.R. White: Phys. Rev. B **43** 8044 (1991).
 - [14] N.E. Bickers, D.J. Scalapino and S.R. White: Phys. Rev. Lett. **62** 961 (1989).
 - [15] H. Kontani and K. Ueda: Phys. Rev. Lett. **80** 5619 (1998).
 - [16] H. Kino and H. Kontani: J. Phys. Soc. Jpn. **67** 3691 (1998).
 - [17] K. Kuroki and H. Aoki: J. Phys. Rev. Lett. **67** 1533 (1998).
 - [18] T. Dahm and L. Tewordt: Phys. Rev. B **52** (1995) 1297.
 - [19] Within the fineness of the \mathbf{k} -mesh.
 - [20] T. Takahashi, *et al.*: J. Phys. Soc. Jpn. **55** 1364 (1986).
 - [21] T. Nakamura, *et al.*: Synth. Met. **70** 1293 (1995).
 - [22] D. Jérôme, *et al.*: Synth. Met. **70** 719 (1995).
 - [23] P. Wzietek, *et al.*: J. Phys. I (France) **3** 171 (1993).
 - [24] M. Takigawa, H. Yasuoka, and G. Saito: J. Phys. Soc. Jpn. **56** 873 (1987).
 - [25] T. Miyazaki, D. Yoshioka, and M. Ogata: Phys. Rev. B **51** 2966 (1995).
 - [26] J.P. Pouget and S. Ravy: J. Phys. I (France), **6** 1501 (1996), J.P. Pouget and S. Ravy: Synth. Met. **85** 1523 (1997).
 - [27] H. Seo and H. Fukuyama: J. Phys. Soc. Jpn. **66** 1249 (1997).
 - [28] N. Kobayashi, M. Ogata and K. Yonemitsu: J. Phys. Soc. Jpn. **67** 1098 (1998).

Fig.1**Fig. 3****Fig. 2****Fig. 4****Fig. 5**